

# Laser-rf double-resonance spectroscopy of refractory elements: $^{183}\text{W I}$ and $^{181}\text{Ta I}$

W. G. Jin, M. Wakasugi, and T. T. Inamura\*

*Cyclotron Laboratory, The Institute of Physical and Chemical Research (RIKEN), Wako, Saitama 351-01, Japan*

T. Murayama

*Tokyo University of Mercantile Marine, Koto, Tokyo 135, Japan*

T. Wakui and H. Katsuragawa

*Department of Physics, Toho University, Funabashi, Chiba 274, Japan*

T. Ariga and T. Ishizuka

*Department of Physics, Saitama University, Urawa, Saitama 338, Japan*

I. Sugai

*Institute for Nuclear Study, University of Tokyo, Tanashi, Tokyo 188, Japan*

(Received 24 January 1994)

Laser-rf double-resonance spectroscopy of  $^{183}\text{W I}$ , an isotope of the most refractory element, has been carried out using an Ar-ion sputtering atomic-beam source; the same technique has been applied to  $^{181}\text{Ta I}$ , another highly refractory element. Hyperfine-interaction constants for the  $5d^46s^2^5D_2$  state in  $^{183}\text{W I}$  and the ground state  $5d^36s^2^4F_{3/2}$  in  $^{181}\text{Ta I}$  have been determined with an order of magnitude better precision than achieved for these refractory elements.

PACS number(s): 32.30.Bv, 35.10.Fk, 42.62.Fi

## I. INTRODUCTION

As is described in a recent overview of laser-radio-frequency double-resonance (LRDR) studies [1], the LRDR technique allows a number of significant advantages in precision, sensitivity, and convenience over the atomic-beam magnetic-resonance (ABMR) technique that has long been well established for the hyperfine-structure study with high precision since the pioneering work of Rabi *et al.* [2]. It should also be mentioned that the setup for the LRDR is much simpler than the one for the ABMR.

Most measurements, however, have been made for nonrefractory elements. Since Dubke *et al.* performed an LRDR measurement on molybdenum isotopes [3], only a few reports on LRDR in refractory elements have been published [4–7]; none for the most refractory element W. So far production of atomic beams of refractory elements has been made by electron bombardment, and as is pointed out by Childs [1], a breakthrough to prevent instabilities inherent in the heating by electron bombardment is much awaited.

We have developed a laser spectroscopic technique using an Ar-ion sputtering atomic-beam source especially to study refractory elements [8,9]. This atomic-beam source is versatile, stable, and very much controllable—so much so that we have succeeded in making a breakthrough in the LRDR technique for the refractory ele-

ment. Here we shall report LRDR spectroscopy of  $^{183}\text{W I}$  as well as the measurement of  $^{181}\text{Ta I}$ .

## II. EXPERIMENTAL SETUP

The present experimental setup is schematically shown in Fig. 1. An Ar-ion sputtering method was used to produce atomic beams of W and Ta. Argon ions generated by an electron gun were accelerated up to 8–10 kV and

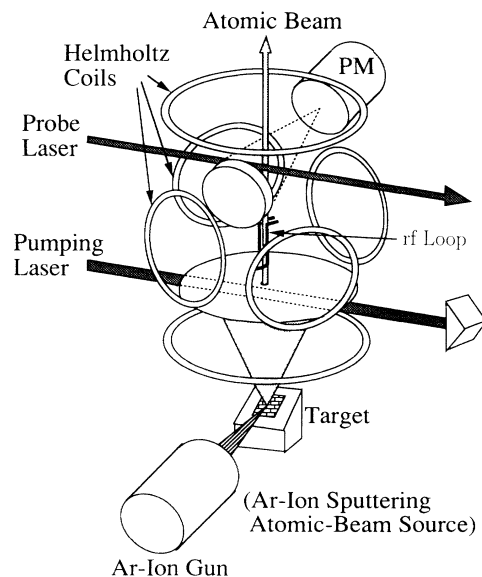


FIG. 1. Experimental setup of laser-rf double-resonance spectroscopy. PM denotes the photomultiplier.

\*Present address: Safety Center, The Institute of Physical and Chemical Research (RIKEN), Wako, Saitama 351-01, Japan.

focused on natural metallic targets of W and Ta. The atomic beams produced by sputtering were collimated with a system consisting of four diaphragms with an aperture of 4 mm in diameter. A typical Ar-ion current was about 0.4 mA, and then the total number of atoms in the collimated beam was about  $10^{11}$  atoms/s.

The laser beam from a ring dye laser (CR 699-29) with rhodamine 110 that was optically pumped by an Ar-ion laser (Spectra Physics 171) was split into two beams, i.e., pumping and probe lasers. The pumping laser to excite atoms in the lower state of the transition had a power of 500 mW in the case of W and 200 mW in the case of Ta; while the probe laser had a power of about 1 mW. Both the pumping and probe lasers were crossed with the collimated atomic beam perpendicularly. The pumping laser was reflected to the opposite direction with a cubic mirror to increase the optical pumping effect. Fluorescence induced by the probe laser was collected and focused on a cooled single-photon counting photomultiplier (Hamamatsu R1333) with a spherical mirror.

A 3-cm-long wire (rf loop) was placed between the two lasers in parallel to the atomic beam to produce an rf field. The radio frequency was generated by a 0–26-GHz synthesizer (HP8341B) and amplified by a 0–500-MHz power amplifier (EIN 510L) for W and a 1–26-GHz power amplifier (HP8348A) for Ta. The rf power applied was typically 30 mW at the terminal connected to the wire. To cancel the stray magnetic field in the rf region, three pairs of Helmholtz coils were used in three dimensions.

### III. RESULT AND DISCUSSION

#### A. Laser-rf double resonance in $^{183}\text{W I}$

A transition of 551.5 nm from the  $5d^46s^2\ ^5D_2$  state to the  $5d^46s6p\ ^7D_1$  state in W I was used in this experiment. First, we measured a laser-induced fluorescence spectrum for the 551.5-nm transition without the pumping laser. The measured fluorescence spectrum of the transition is shown in Fig. 2. The full width at half maximum (FWHM) of the peaks was about 45 MHz. Assignments of the hyperfine peaks of  $^{183}\text{W}$  whose nuclear spin is  $\frac{1}{2}$  are indicated in the energy level diagram of the hyperfine splittings of the lower  $^5D_2$  and upper  $^7D_1$  states.

In the LRDR measurement, the laser frequency was fixed at the hyperfine peak (2), i.e., the strongest transition  $F = \frac{5}{2}(^5D_2) - \frac{3}{2}(^7D_1)$ . (See Fig. 2.) The population of the lower  $F = \frac{5}{2}$  hyperfine level was thereby strongly depleted by the pumping laser; the fluorescence intensity induced by the probe laser only was reduced by 90%. Then radio frequency was applied to repopulate the depleted  $F = \frac{5}{2}(^5D_2)$  state at a frequency that coincided with the hyperfine splitting of the  $^5D_2$  state; the fluorescence regained its intensity up to 90% of the one observed for the probe laser only, depending on the transitions. We observed the change of the fluorescence intensity as a function of rf by scanning the rf applied to the rf loop.

There was a stray magnetic field of about 300 mG at the rf region without applying the Helmholtz coils. In this case, two hyperfine levels with  $F = \frac{5}{2}$  and  $\frac{3}{2}$  in  $^5D_2$  are

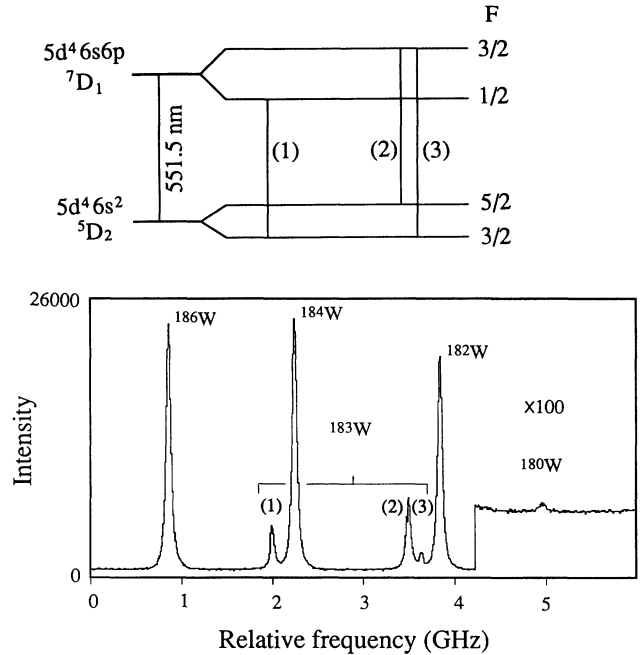


FIG. 2. Laser-induced fluorescence intensity (counts/s) of the 551.5-nm ( $^5D_2$ - $^7D_1$ ) transition in W I. Peaks of even-mass isotopes are labeled with isotopic symbols. Assignments of hyperfine peaks of  $^{183}\text{W}$  and hyperfine splittings of the lower  $^5D_2$  and upper  $^7D_1$  states are shown in the energy level diagram.

split into Zeeman sublevels, respectively, as shown in Fig. 3(a). A measured rf-resonance spectrum in the stray magnetic field is shown with open circles in Fig. 3(b). By calculating the Zeeman-splitting energies using the known electronic  $g$  factor  $g_J = 1.48683(8)$  of the  $^5D_2$  state [10], these resonances were exactly assigned as shown in the figure. When the stray field was canceled out by an external magnetic field produced with the Helmholtz coils in three dimensions, a single-resonance peak was observed as expected for a near-zero field. [Closed circles in Fig. 3(b)].

The hyperfine splitting of  $F = \frac{3}{2} - \frac{5}{2}$  in the  $5d^46s^2\ ^5D_2$  state of  $^{183}\text{W I}$  was determined by making a least-squares fit of a Lorentzian function to the experimental rf-resonance spectrum at the near-zero field. The hyperfine magnetic interaction constant  $A$  for the  $^5D_2$  state was then derived as is listed in Table I; the one obtained by means of the ABMR [11] is also presented for comparison. The precision of the present measurement is an order of magnitude better than the latter. The hyperfine splitting in the state derived from the center of gravity of the Zeeman splitting at the stray magnetic field agrees with the value obtained from the single-resonance peak at the near-zero field.

The experimental FWHM of the measured rf-resonance peak of  $^{183}\text{W I}$  at the near-zero field was 200 kHz. Such a peak width for the rf-resonance peak arises from the limited transit time of atoms in the rf field and the residual Zeeman broadening caused by the remnant magnetic field in the rf region. By taking into account the velocity distribution and geometrical effect of the sputtered W atoms [8], the contribution from the transit

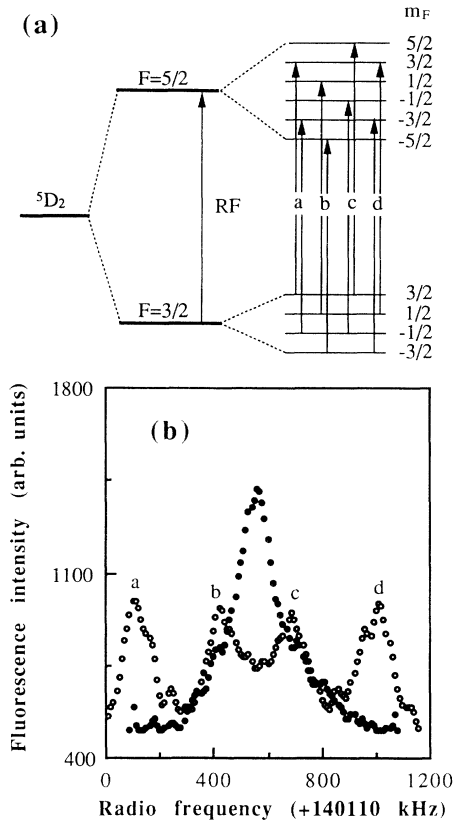


FIG. 3. (a) Hyperfine and Zeeman splittings, and rf transitions between Zeeman sublevels for the  $5d^4 6s^2 5D_2$  state in  $^{183}\text{W I}$  and (b) measured rf-resonance spectrum for the  $F = \frac{3}{2} - \frac{5}{2}$  hyperfine splitting of the  $5D_2$  state. Open circles show the spectrum observed in a stray magnetic field of about 300 mG and closed ones the spectrum in a near-zero field.

time is calculated to be about 105 kHz using the formula of the rf-transition probability [12]. This is still smaller than the measured one. This discrepancy is considered to be caused by a remnant magnetic field in the rf region, which is estimated to be about 50 mG.

#### B. Laser-rf double resonance in $^{181}\text{Ta I}$

A group at Göteborg made LRDR measurements of highly excited metastable states in  $^{181}\text{Ta I}$  by electron bombardment [6,7]. Here we chose a 540.3-nm transition from the ground state  $5d^3 6s^2 4F_{3/2}$  to the  $5d^2 6s^2 6p 4D_{1/2}$  state in Ta I because the high-lying states were less populated in sputtered atoms [8]. A measured fluorescence spectrum for the 540.3-nm transition is shown in Fig. 4. Assignments of the hyperfine peaks of  $^{181}\text{Ta}$  whose nuclear spin is  $\frac{7}{2}$  are indicated in the energy level diagram of the hyperfine splittings of the lower  $4F_{3/2}$  and upper  $4D_{1/2}$  states. The six hyperfine transitions were all observed though two peaks (3) and (4) overlapped. The FWHM of the peaks was about 40 MHz.

The measured rf-resonance spectra for the lower  $4F_{3/2}$  state at the near-zero field are shown in Fig. 5(a) for the hyperfine splitting of  $F=4-5$ , in 5(b) for  $F=3-4$ , and in 5(c) for  $F=2-3$ ; the laser frequency was fixed at the hyperfine transitions of (1)  $F=5(4F_{3/2})-4(4D_{1/2})$ , (5)

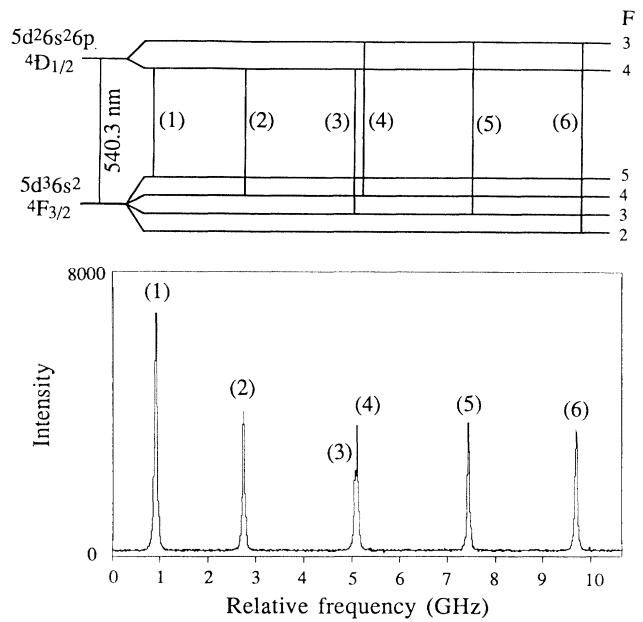


FIG. 4. Laser-induced fluorescence intensity (counts/s) of the 540.3-nm ( $4F_{3/2} - 4D_{1/2}$ ) transition in Ta I. Assignments of hyperfine peaks of  $^{181}\text{Ta}$  and hyperfine splittings of the lower  $4F_{3/2}$  and upper  $4D_{1/2}$  states are shown in the energy level diagram.

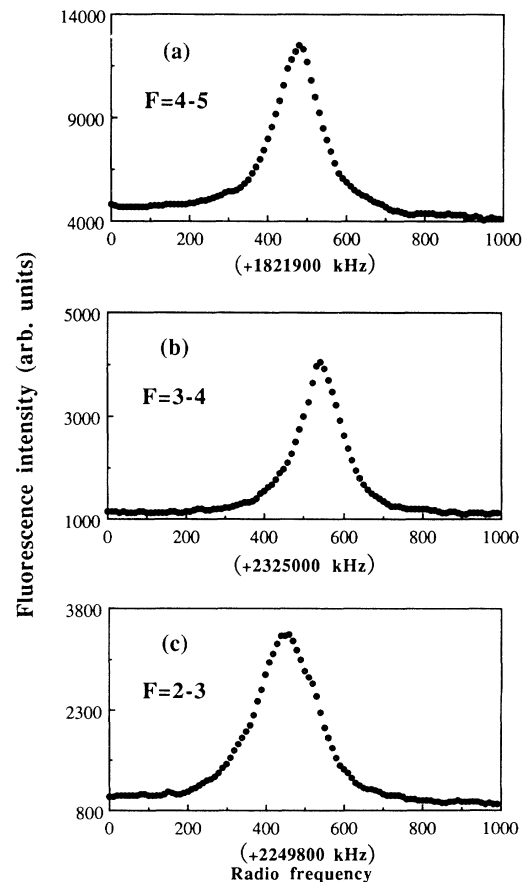


FIG. 5. Measured rf-resonance spectra for the hyperfine splittings of (a)  $F=4-5$ , (b)  $F=3-4$ , and (c)  $F=2-3$  for the ground state  $5d^3 6s^2 4F_{3/2}$  in  $^{181}\text{Ta I}$ .

TABLE I. Determined hyperfine splittings and constants  $A$  and  $B$  for the  $5d^46s^2^5D_2$  state in  $^{183}\text{W I}$  and the ground state  $5d^36s^2^4F_{3/2}$  in  $^{181}\text{Ta I}$ .

Isotope	Nuclear		Hyperfine level ( $F-F'$ )	Hyperfine splitting (MHz)	$A, B$ (MHz)	
	spin	State			Present (LRDR)	Previous (ABMR)
$^{183}\text{W}$	$\frac{1}{2}$	$5d^46s^2^5D_2$	$\frac{3}{2}-\frac{5}{2}$	140.670(2)	$A = 56.268\ 1(8)$	$56.261(8)^a$
			2-3	2250.2555(7)	$A = 509.081\ 03(9)$	$509.0821(8)^b$
$^{181}\text{Ta}$	$\frac{7}{2}$	$5d^36s^2^4F_{3/2}$	3-4	2325.5401(6)	$B = -1012.228\ 2(6)$	$-1012.230(8)^b$
			4-5	1822.3832(5)		

<sup>a</sup>Reference [11].

<sup>b</sup>Reference [13].

$F=3-3$ , and (6)  $F=2-3$ , respectively. From the measured rf-resonance spectra in Ta I, the three hyperfine splittings in the  $5d^36s^2^4F_{3/2}$  state were determined. The magnetic interaction constant  $A$  and electric interaction constant  $B$  were thus derived for the  $^4F_{3/2}$  state. The results are listed in Table I; those obtained by means of the ABMR [13] are presented for comparison. The present precision is again an order of magnitude better than the latter. The FWHM of the measured rf-resonance peak of  $^{181}\text{Ta}$  is about 105 kHz and is in good agreement with the one calculated for zero-magnetic field from the transit time of atoms in the rf field. (See Sec. III A). This is consistent with the fact that the residual Zeeman broadening is very small because of the small electronic  $g$  factor  $g_J=0.450\ 24(4)$  of the  $^4F_{3/2}$  state [14].

The FWHM of the rf-resonance peak obtained in the present experiment is several times larger than that of 10–20 kHz usually observed for the thermal atomic beam [1] when statistics of the data are comparable with that of the present measurement. Since the peak width is determined mainly by the transit time of atoms in the rf field [12], this is reasonable because the velocity of the sputtered atoms is several times larger than that of the thermal atoms [8], i.e., the sputtered atoms have less

transit time for the same-length rf loop. However, the sputtering atomic-beam source has a great advantage over the electron bombardment one. There is no such instabilities as one encounters in heating up the refractory elements by electron bombardment. Sputtering is not a thermal process, but a rapid dynamical process; it is highly stable and controllable [8].

In summary, using an Ar-ion sputtering atomic-beam source, we have successfully made laser-rf double-resonance spectroscopy of  $^{183}\text{W I}$ , an isotope of the most refractory element. We have also made a high-precision hyperfine measurement of  $^{181}\text{Ta I}$ . The hyperfine constant  $A$  of  $^{183}\text{W I}$  for the  $5d^46s^2^5D_2$  state and constants  $A$  and  $B$  of  $^{181}\text{Ta I}$  for the  $5d^36s^2^4F_{3/2}$  state have been determined.

#### ACKNOWLEDGMENTS

The authors would like to thank Dr. Y. Yano at RIKEN for his constant support of this study. Thanks are also due to Dr. K. Morita for his comments and enlightening discussions. One of us (W.G.J.) would like to acknowledge the Special Researchers' Basic Science Program.

- [1] W. J. Childs, Phys. Rep. **211**, 113 (1992).  
 [2] I. I. Rabi, J. R. Zacharias, S. Millman, and P. Kusch, Phys. Rev. **53**, 318 (1938).  
 [3] M. Dubke, W. Jitschin, G. Meisel, and W. J. Childs, Phys. Lett. **65A**, 109 (1978).  
 [4] G. Olsson, T. Olsson, L. Robertsson, and A. Rosén, Phys. Scr. **29**, 61 (1984).  
 [5] L. Fraenkel, C. Bengtsson, D. Hanstorp, A. Nyberg, and J. Persson, Z. Phys. D **8**, 171 (1988).  
 [6] J. Persson, U. Berzinsh, T. Nilsson, and M. Gustavsson, Z. Phys. D **23**, 67 (1992).  
 [7] U. Berzinsh, M. Gustafsson, and J. Persson, Z. Phys. D **27**, 155 (1993).  
 [8] M. Wakasugi, W. G. Jin, T. T. Inamura, T. Murayama, T. Wakui, T. Kashiwabara, H. Katsuragawa, T. Ariga, T. Ishizuka, M. Koizumi, and I. Sugai, Rev. Sci. Instrum. **64**, 3487 (1993).  
 [9] W. G. Jin, M. Wakasugi, T. T. Inamura, T. Murayama, T. Wakui, H. Katsuragawa, T. Ariga, T. Ishizuka, M. Koizumi, and I. Sugai, Phys. Rev. A **49**, 762 (1994).  
 [10] S. Büttgenbach, R. Dicke, and F. Träber, Phys. Rev. A **19**, 1383 (1979).  
 [11] S. Büttgenbach, R. Dicke, H. Gebauer, R. Kuhnen, and F. Träber, Z. Phys. A **283**, 303 (1977).  
 [12] N. F. Ramsey, *Molecular Beams* (Oxford University Press, New York, 1956), p. 118.  
 [13] S. Büttgenbach and G. Meisel, Z. Phys. **244**, 149 (1971).  
 [14] K. H. Bürger, S. Büttgenbach, R. Dicke, H. Gebauer, R. Kuhnen, and F. Träber, Z. Phys. A **298**, 159 (1980).

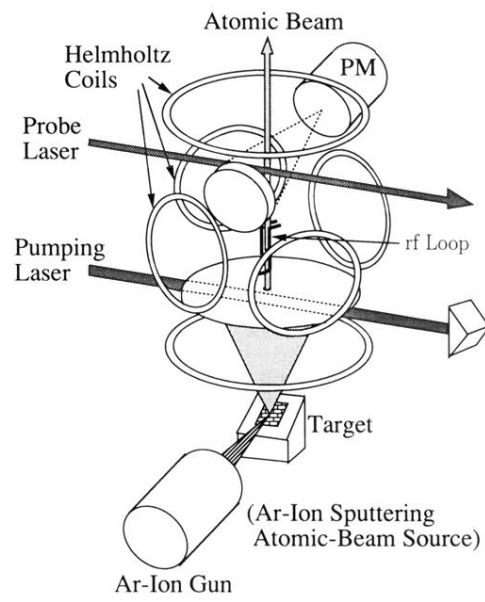


FIG. 1. Experimental setup of laser-rf double-resonance spectroscopy. PM denotes the photomultiplier.